Experimental Brain Research (2020) 238:2581–2588
https://doi.org/10.1007/s00221-020-05918-4

RESEARCH ARTICLE

Functional specialization in human dorsal pathway for stereoscopic depth processing

Nihong Chen[1,2] · Zhimin Chen[3] · Fang Fang[3,4,5,6]

Received: 14 April 2020 / Accepted: 1 September 2020 / Published online: 4 September 2020

Abstract

Binocular disparity, a primary cue for stereoscopic depth perception, is widely represented in visual cortex. However, the functional specialization in the disparity processing network remains unclear. Using magnetic resonance imaging-guided transcranial magnetic stimulation, we studied the causal contributions of V3A and MT+ to stereoscopic depth perception. Subjects viewed random-dot stereograms forming transparent planes with various interplane disparities. Their smallest detectable disparity and largest detectable disparity were measured in two experiments. We found that the smallest detectable disparity was affected by V3A, but not MT+ , stimulation. On the other hand, the largest detectable disparity was affected by both V3A and MT+ stimulation. Our results suggest different roles of V3A and MT+ in stereoscopic depth processing.

Keywords Depth perception · Binocular disparity · Transcranial magnetic stimulation · Continuous theta burst stimulation

Introduction

We perceive the three-dimensional world from two-dimensional images projected onto the two retinas. Binocular disparity, the positional difference between the left and right retinal images, provides a sufficient cue to evoke stereoscopic depth perception (Wheatstone 1838). Random dot stereograms, which take advantage of binocular disparity information, have been widely used to unravel the cortical mechanisms of stereoscopic depth perception with psychophysical, physiological, and computational methods (Qian 1997; Cumming and DeAngelis 2001; Parker 2007). After a point-to-point matching of local dots in the left and right eyes, the spread of disparity information "fills in" the depth for blank space between dots, giving rise to a perception of surface or figure-ground segmentation based on disparity (Julesz 1960; Westheimer 1986; Parker and Yang 1989) (Fig. 1a).

The response of a substantial proportion of visual neurons depends critically on the binocular disparity (Poggio 1995). Compared to zero-disparity stimuli, disparity-rich stimuli evoked greater activation in multiple regions along the dorsal and ventral streams (Tsao et al. 2003; Neri et al. 2004; Minini et al. 2010). It has been suggested that dorsal areas encode the metric magnitude of disparity, while the ventral areas signal disparity in a categorical manner (Preston et al. 2008; Cottereau et al. 2011).

In the dorsal stream, MT+ and V3A have been mostly studied for disparity processing. As a well-known area for visual motion, MT+ has been long discovered to have disparity-tuned neurons in macaques (Maunsell and van Essen 1983; DeAngelis and Newsome 1999; Roy et al. 1992). However, MT+ only established moderate disparity

Communicated by Melvyn A. Goodale.

Nihong Chen and Zhimin Chen have contributed equally to this work.

✉ Nihong Chen
nihongch@tsinghua.edu.cn

✉ Fang Fang
ffang@pku.edu.cn

1 Department of Psychology, School of Social Sciences, Tsinghua University, Beijing 100084, China

2 THU-IDG/McGovern Institute for Brain Research, Beijing 100084, China

3 School of Psychological and Cognitive Sciences, Peking University, Beijing 100871, China

4 Beijing Key Laboratory of Behavior and Mental Health, Beijing, China

5 PKU-IDG/McGovern Institute for Brain Research, Beijing, China

6 Peking-Tsinghua Center for Life Sciences, Peking University, Beijing 100871, China

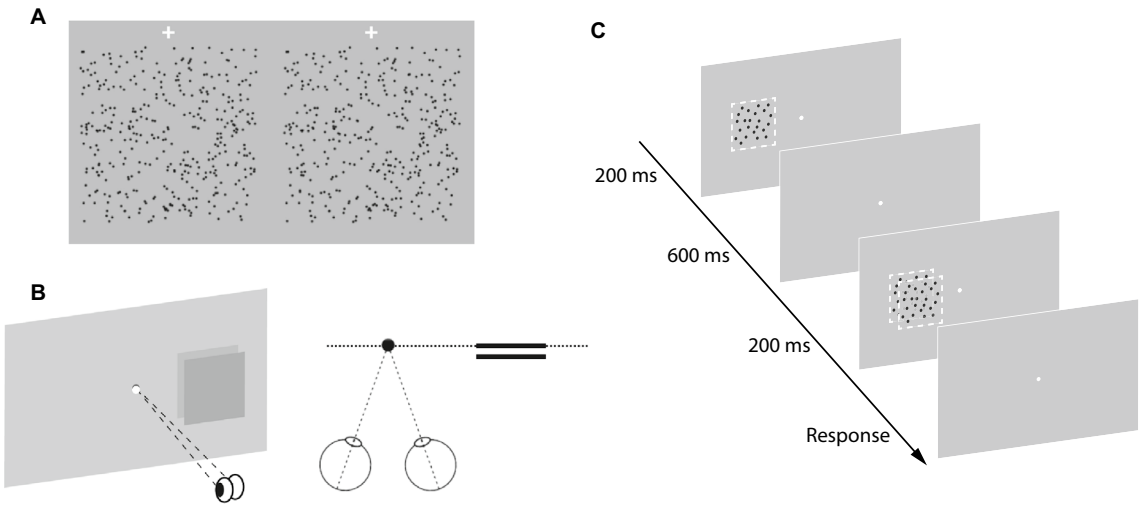

Fig. 1 **a** Random-dot stereograms used to form a perception of two transparent planes. The white crosses at the top only appeared in the illustrative figure to aid free fusion. **b** Schematic illustration of the experimental stimuli. **c** 2-AFC trial in the stereoacuity task. Dashed frames indicate the region of a disparity-defined plane

selectivity in humans (Tsao et al. 2003; Rutschmann and Greenlee 2004). In contrast, V3A received a lot of interest in human disparity research. It has been found V3A showed the strongest effect of disparity modulation on fMRI BOLD signals (Tsao et al. 2003). Also, the neural code in V3A has a close relationship with functional characteristics of stereoscopic depth perception (Goncalves et al. 2015). Specifically, Backus et al. (2001) compared human psychophysical thresholds with fMRI BOLD responses in two tasks. In a stereoacuity test, subjects were asked to detect the disparity-defined double planes from a zero-disparity plane. They found that V3A had a higher sensitivity than other visual areas including MT+. In the other test, subjects were asked to detect the disparity-defined planes from uncorrelated dots to determine their upper disparity limit. They found that area V3A, together with MT+, demonstrated the highest sensitivity in extrastriate visual cortex.

In spite of the disparity-selective response, a few studies have directly tested the causal contributions of V3A and MT+ in stereoscopic depth processing. Here, we adopted the random-dot stereograms and tasks used by Backus et al. (2001) with off-line continuous theta burst stimulation (cTBS) which transiently attenuates normal cortical function (Huang et al. 2005; van Kemenade et al. 2012). Functional mapping was used to localize V3A and MT+ in individual subjects and to guide cTBS delivery. Disparity thresholds were compared before and after cTBS, and stimuli were presented contralateral or ipsilateral to the stimulation site. The vertex was also targeted as a control reference.

In the present study, the first experiment tested the lower disparity limit in which subjects were asked to discriminate stereograms from zero disparity, and the second experiment tested the upper disparity limit in which subjects were asked to discriminate stereograms from uncorrelated dots. Based on a previous brain imaging study with similar stimuli and tasks (Backus et al. 2001), we hypothesized that the lower limit disparity processing depends primarily on V3A, and the upper limit disparity processing depends on both V3A and MT+.

Materials and methods

Subjects

Ten (five females) participated in Experiment 1 for the lower limit (stereoacuity) test. Ten subjects (four females) participated in Experiment 2 for the upper limit test. All were neurologically healthy and had normal or corrected-to-normal visual acuity. They gave written, informed consent in accordance with the procedures and protocols approved by the human subject review committee of Peking University.

Stimuli and apparatus

Stimuli were random-dot stereograms containing 200 black dots (luminance, 0.052 cd/m^2; diameter, 0.1°) on a gray background (luminance, 12.56 cd/m^2) within an 8° × 8° square region at a horizontal eccentricity of 8° either left or right from the center. Dots were assigned to one of two planes in depth by adding horizontal disparities to the dots (Fig. 1b). As the depth between the planes increased, one saw first a single plane of dots, then a thickened plane (±0.25 arcmin to ±1 arcmin), and then two distinct planes

(> 1 arcmin). As the disparity increased and approached ~ 70 arcmin, the two distinct planes became indistinguishable from dots that were placed uncorrelated in the two eyes' images (Backus et al. 2001). The left and right 2° margins of the displays contained binocularly uncorrelated dots, so that both the width of the binocular images were kept constant across disparities. The fixation point was a white dot (luminance, 103.56 cd/m^2) presented at the center of the screen with a diameter of 0.2° at zero disparity.

The stimuli were generated and presented using MATLAB (MathWorks) with Psychtoolbox-3 (Brainard 1997). Stimuli were displayed on a Viewsonic VX2268wm LCD monitor at 120 Hz with screen resolution of 1680 × 1050 pixels. Stereoscopic presentation was controlled by Nvidia GeForce 3D Vision glasses with shutters that alternated at 120 Hz synchronized with the monitor, updating at 60 Hz per eye. Subjects viewed the stimuli at a distance of 60 cm with their heads stabilized by a head and chin rest and were asked to fixate at this point throughout the experiment.

Experimental procedure

Subjects' disparity thresholds were measured using two-alternative forced choice (2-AFC) method. Experiment 1 tested the lower limit of disparity. In a trial, one stimulus interval consisted of a two-plane stereogram and the other consisted of a one-plane stereogram (i.e., zero interplane disparity) (Fig. 1c). Subjects reported which interval contained a two-plane stimulus by a key press. Experiment 2 tested the upper limit of disparity. In a trial, one stimulus interval consisted of a two-plane stereogram with a large disparity (above 10 arcmin), and the other consisted of dots at positions uncorrelated between the left and right retinal images. Subjects reported which interval contained a two-plane stimulus by a key press.

In both experiments, each stimulus was presented for 200 ms, with a 600 ms blank. The order of the two stimuli was randomized across trials. Informative feedback was provided after each key press by brightening (correct) or dimming (wrong) the fixation point. The next trial began 1 s after feedback. In each test phase, subjects completed five QUEST staircases of 40 trials (Watson and Pelli 1983) to estimate 75% correct threshold in the left and the right visual field.

MRI data acquisition

MRI scan was performed using a 3-T Siemens Trio scanner with a 12-channel phased array head coil. Blood-oxygenation-level-dependent (BOLD) signals were measured with an EPI sequence [33 axial slices, repetition time (TR) = 2 s, echo time (TE) = 30 ms, voxel size = 3 × 3 × 3 mm^3, and no interslice gap]. A high-resolution 3D structural data set (T1-weighted MPRAGE, 1 × 1 × 1 mm^3 resolution) was acquired in the same session.

Functional localization of V3A and MT+

Retinotopic visual areas V1, V2, V3, and V3A were defined using a standard phase-encoded paradigm (Sereno et al. 1995; Engel et al. 1997), in which subjects viewed a rotating wedge and an expanding ring that created traveling waves of neural activity in visual cortex. Independent block-design runs were conducted to localize the region of interests (ROIs) in V3A and MT+. Each run consisted of ten 12 s moving dot blocks interleaved with 12 s stationary dot blocks. For each block, 400 dark dots (luminance: 0.021 cd/m^2; diameter: 0.1°) were presented against a gray background (luminance: 11.55 cd/m^2), within an area subtending 8° in diameter. The center of the aperture was positioned 8° horizontally to the left or right of the central fixation point. In the moving dot blocks, each dot traveled back and forth along a randomly chosen direction, alternating once per second.

FMRI data were processed using BrainVoyager QX (Brain Innovation). The anatomical volume for each subject was transformed into the AC-PC space and then inflated. Functional volumes for each subject were preprocessed, including 3D motion correction, linear trend removal, and high-pass (0.015 Hz) filtering. The functional volumes were then aligned to the anatomical volume. MT+ is a visual area responsive to moving stimuli within or near the occipital continuation of the inferior temporal sulcus. The ROIs in V3A and MT+ in each hemisphere were defined as voxels that responded more strongly to moving dots in the contralateral visual hemifield than to those in the ipsilateral visual hemifield ($p < 0.001$, uncorrected) (Cai et al. 2014).

TMS

Continuous theta burst stimulation (cTBS) was delivered through a MagStim Super Rapid^2 stimulator (MagStim, Whitland, UK) with a double 70-mm figure-of-eight coil. We used a classical off-line protocol, which has been shown to induce cortical suppression for up to 60 min (Huang et al. 2005; Allen et al. 2007). Specifically, a train of 600 pulses, 3 pulses at 50 Hz every 200 ms, was delivered at 50% of the maximum stimulator output. The same protocol has been applied at V3A and MT+, and has been shown to impair visual motion discrimination (Cai et al. 2014).

Individual structural and functional MRI data were imported in Visor2 neuro-navigation system (Advanced Neuro Technology, The Netherlands) to provide real-time stimulation guidance. The center of gravity for each ROI was defined as the stimulation site (Fig. 2). The coil was held over the scalp tangentially with the handle directing

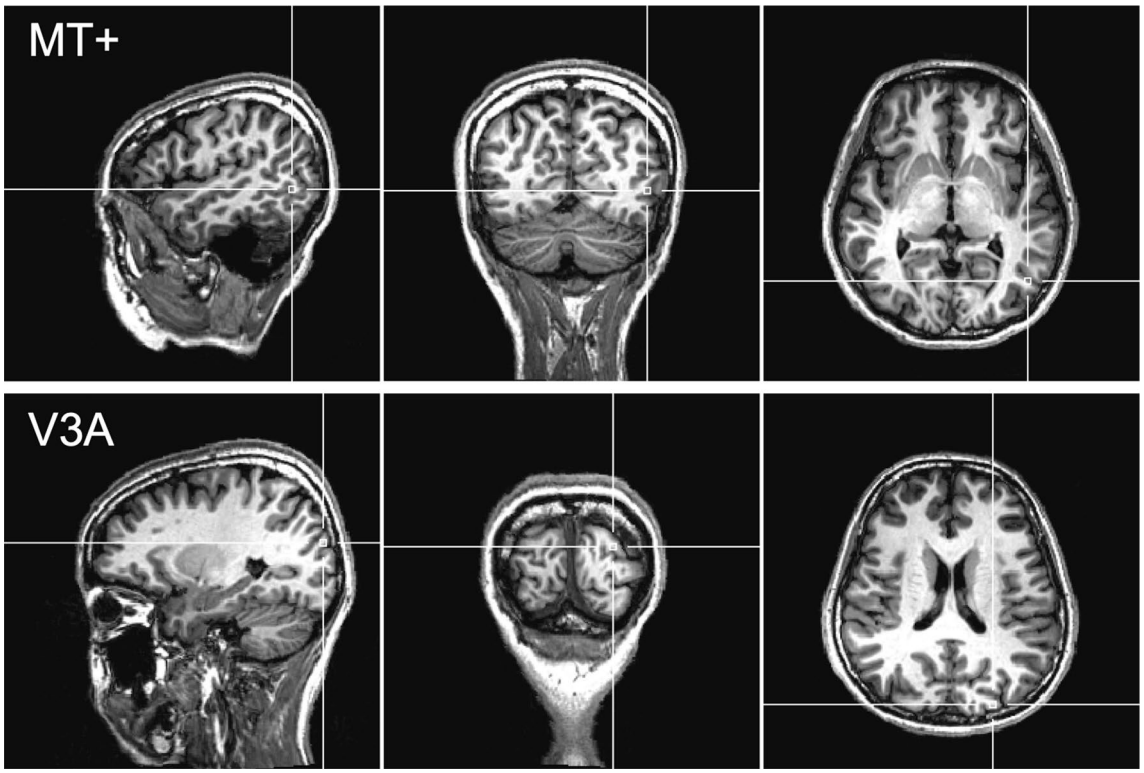

Fig. 2 TMS site at V3A and MT+ of a representative subject. The cross indicates the center of gravity of each ROI

posterior toward the occiput parallel to the subject's spine. The position of the coil was monitored in real time through the course of the 40 s cTBS protocol. The vertex, a site half way between the intertragal notches served as the control site. Each subject received stimulation over unilateral V3A, MT+, and vertex in three sessions. The stimulation hemisphere was randomly determined in each subject, and the stimulation order of the three cortical sites was counterbalanced across subjects. Each session was separated by at least 24 h (Carmel et al. 2010; Cocchi et al. 2015).

Results

Experiment 1 measured subjects' lower disparity limit, i.e., the minimum disparity for perceiving the stereograms as two planes rather than one single plane. An increase in the threshold was associated with a deteriorated performance (Fig. 3). In a daily session, subjects received stimulation over unilateral V3A or MT+. We first compared subjects' stereoscopic thresholds before and after cTBS using a repeated-measures ANOVA with stimulation site (V3A/MT +), visual field (contralateral/ipsilateral), and test (pre-TMS/post-TMS) as independent factors. A significant interaction effect [$F(1, 9) = 7.80$, $p < 0.05$] was revealed, indicating that the lower disparity limit was modulated by cTBS, stimulation site, and visual field. Next, we performed a two-way repeated-measures ANOVA for each visual area with Bonferroni correction. In the V3A stimulation condition, there was a significant interaction between test and visual field [$F(1, 9) = 38.25$, $p < 0.01$]. The threshold increased in the contralateral [paired t test, $t(9) = 3.19$, $p < 0.05$], but not in the ipsilateral visual field [$t(9) = 1.97$, $p > 0.05$]. This location-specific change indicates a disruptive effect. In other words, subjects' stereoacuity performance dropped—a larger disparity was needed to differentiate two planes from one single plane after cTBS. In the MT⇓← stimulation condition, the interaction between test and stimulus position was not significant [$F(1, 9) = 1.03$, $p > 0.05$]. Also, we stimulated the vertex—a location in the middle of the scalp and the visual field could not be categorized as ipsilateral or contralateral. For this control condition, we averaged the thresholds across visual fields. No threshold change was observed before and after TMS [$t(9) = 1.62$, $p > 0.05$].

The TMS effect was quantified as (pre-TMS threshold − post-TMS threshold)/pre-TMS threshold × 100% (Fig. 3, right panel). A value larger than zero indicates facilitation, and a value smaller than zero indicates disruption. The indices were submitted to a two-way repeated-measures ANOVA with stimulation site (V3A/MT+) and visual field (contralateral/ipsilateral) as two within-subject factors. The location-specific TMS effect was different between the two

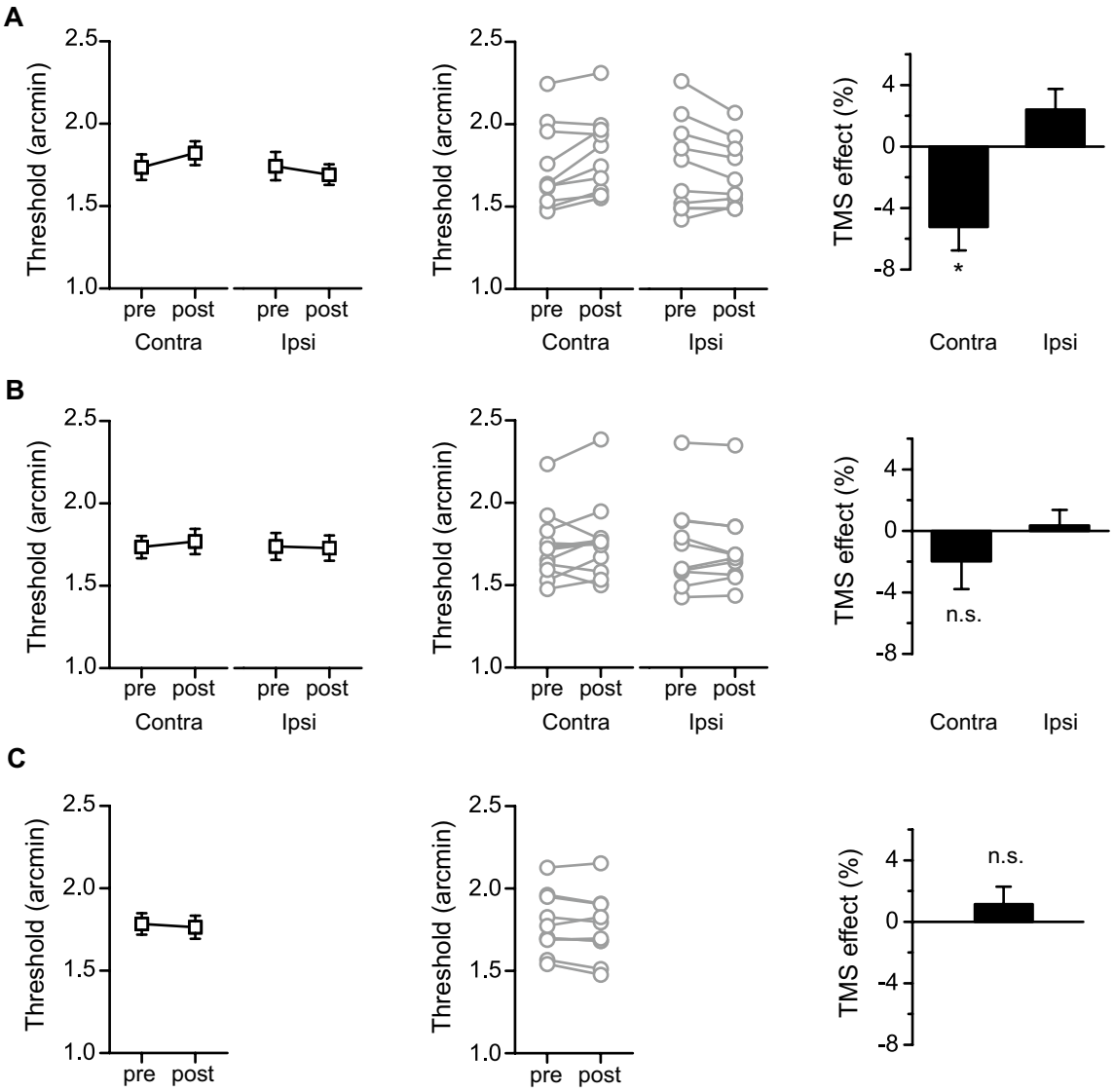

Fig. 3 TMS effects in the lower limit task. TMS effects at **a** V3A, **b** MT+, and **c** vertex. Left panel: averaged thresholds before and after stimulation; middle panel: individual thresholds pre- and post-stimulation; right panel: stimulation effects quantified in percentage change. A value greater than zero indicates facilitation, and a value below zero indicates disruption. *$p < 0.05$ after Bonferroni correction. Error bars denote 1 standard error of mean across subjects

stimulation sites as indicated by a significant interaction effect [$F(1, 9) = 6.92$, $p < 0.05$]. Compared to the ipsilateral visual field, the disruptive effect in the contralateral visual field was significant in the V3A stimulation condition [$t(9) = 6.18$, $p < 0.01$], but not in the MT+ stimulation condition [$t(9) = 0.93$, $p > 0.05$].

Experiment 2 measured subjects' upper disparity limit, i.e., the maximum disparity for perceiving the stereograms as superimposed planes rather than uncorrelated dots. A decrease in the threshold was associated with a deteriorated performance (Fig. 4). Subjects' stereoscopic thresholds before and after cTBS were submitted to a three-way repeated-measures ANOVA. A significant interaction between test and stimulation site was found [$F(1, 9) = 6.19$, $p < 0.05$]. Next, we performed a two-way repeated-measures ANOVA for each visual area with Bonferroni correction. The interaction between test and visual field was significant in both the V3A [$F(1, 9) = 16.98$, $p < 0.05$] and the MT+ [$F(1, 9) = 12.06$, $p < 0.01$] stimulation conditions. In both conditions, the threshold decreased in the contralateral visual field [both $t(9) > 3.05$, $p < 0.05$], but not in the ipsilateral visual field [both $t(9) < 1.04$, $p > 0.05$]. This location-specific change indicates a disruptive effect. In other words, after cTBS, subjects were not able to integrate binocular disparity as large as before to perceive

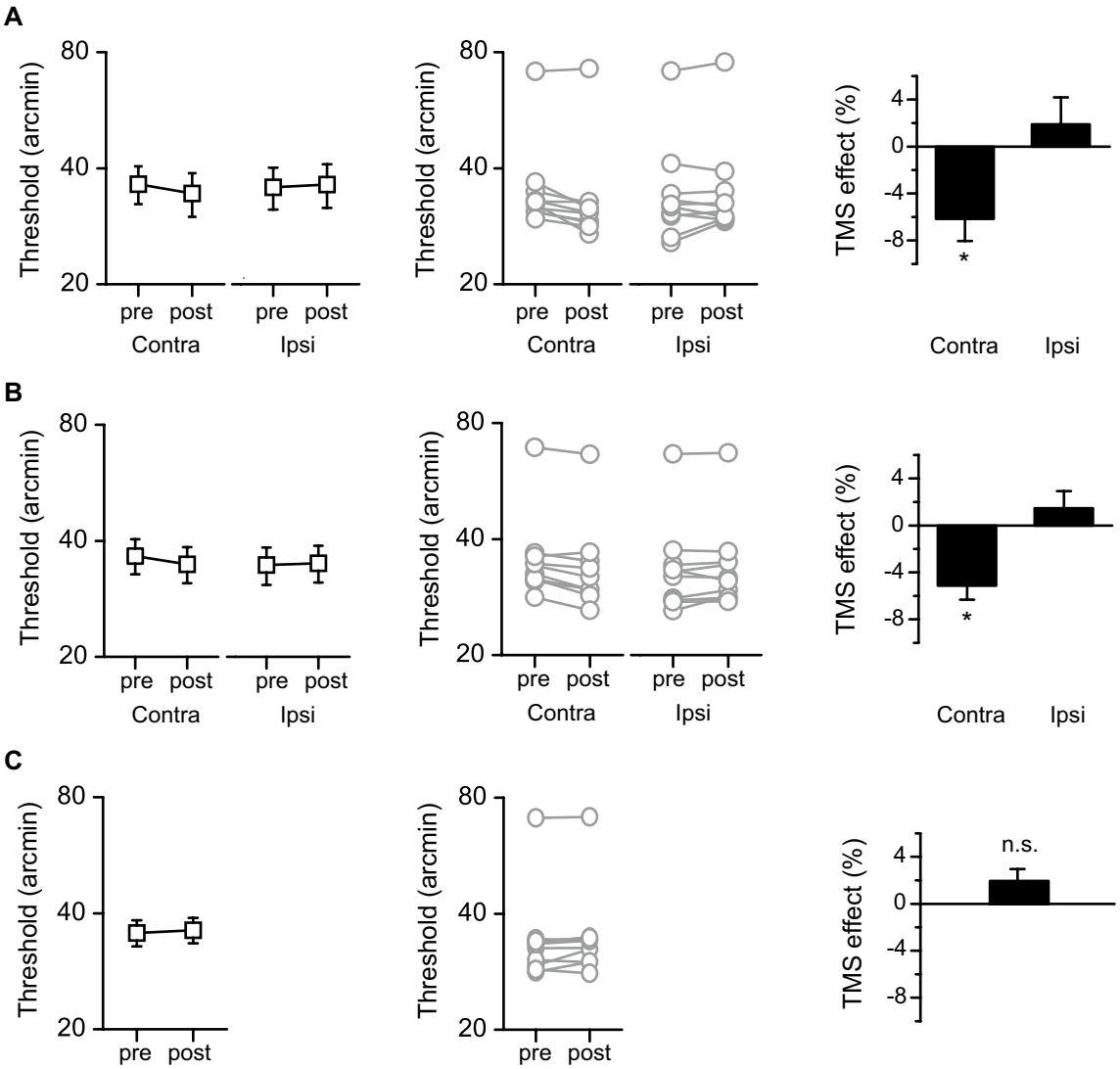

Fig. 4 TMS effects in the upper limit task. TMS effects at **a** V3A, **b** MT+, and **c** vertex. Left panel: averaged thresholds before and after stimulation, shown in a logarithmic scale; middle panel: individual thresholds before and after stimulation, shown in a logarithmic scale; right panel: stimulation effects quantified in percentage change. A value greater than zero indicates facilitation, and a value below zero indicates disruption. *$p < 0.05$ after Bonferroni correction. Error bars denote 1 standard error of mean across subjects

superimposed planes. In the vertex stimulation condition, no threshold change was observed [$t(9) = 1.66$, $p > 0.05$].

The TMS effect was further quantified as (post-TMS threshold − pre-TMS threshold)/pre-training threshold × 100%. A value larger than zero indicates facilitation, and a value smaller than zero indicates disruption (Fig. 4b). The indices were submitted to repeated-measures ANOVA with TMS site (V3A/MT+) and visual field (contralateral/ipsilateral) as two within-subject factors. A location-specific TMS effect was indicated by a significant visual field effect [$F(1, 9) = 7.47$, $p < 0.05$]. Post hoc t test showed a significant disruptive effect in the contralateral visual field compared to the ipsilateral visual field in both the V3A [$t(9) = 2.75$, $p < 0.05$] and the MT+ [$t(9) = 3.27$, $p < 0.01$] stimulation conditions. However, the interaction effect was not significant [$F(1, 9) = 0.03$, $p > 0.05$], suggesting that the location-specific effect did not differ between the V3A and MT+ stimulation conditions.

Discussion

The present study investigated the functional specialization of areas V3A and MT+ in stereoscopic processing. We found that stimulation at V3A, but not MT+, impaired the lower disparity limit, suggesting a unique role of V3A in stereoacuity processing. On the other hand, V3A or MT+ stimulation both impaired the upper disparity limit, suggesting

that both V3A and MT+ contribute in binocular integration for large disparity.

First, our TMS results suggest that V3A has a causal contribution in perceiving both the lower and the upper disparity limits. The previous human fMRI studies have demonstrated that the BOLD signal in V3A was highly sensitive to disparity magnitude, with organized structure correlated with stereoscopic perceptual judgments (Goncalves et al. 2015). Using similar random-dot stereograms forming planes with various interplane disparities, Backus et al. (2001) found that the disparity-related response increased as the interplane disparity increased from undetectable to detectable, and decreased sharply after exceeding the upper depth limit. The covariation between cortical response and perceptual threshold suggests that V3A is an important neural substrate of stereoscopic depth perception.

Second, we found that TMS at MT+ impaired subjects' upper disparity threshold. This is consistent with the long-established link between MT and stereoscopic vision. Macaque studies have demonstrated that MT inactivation affected extracting a disparity-defined target from noise (DeAngelis et al. 1998; Uka and DeAngelis 2003). Specifically, MT inactivation only impaired the coarse judgment of disparities in noise, but not the fine discrimination of disparities (Uka and DeAngelis 2006; Chowdhury and DeAngelis 2008). Such "fine" versus "coarse" functional specialization between V3A and MT+ has also been found in other visual processes such as local versus global motion (Cai et al. 2014).

The functional specialization revealed in the current study may be explained by a higher sensitivity of V3A in encoding disparity near the lower limit. Early psychophysical studies suggested that the relative disparity provides a crucial cue for stereoscopic depth discrimination (Kumar and Glaser 1992; Westheimer 1979). A steady-state EEG study with fMRI localization examined the population-response dynamics that are evoked by periodically changing disparities in five visual regions of interest (V1, MT+, V4, LOC, and V3A). By comparing responses between the absolute and the relative disparity conditions, Cottereau et al. (2011) found that V3A was the only region exhibiting significant changes both in the response amplitude and the phase lag. These converging evidence from psychophysical, electrophysiological, and brain imaging studies point to a distinct role of V3A for differentiating fine disparity signals.

It should be noted that the type of stimuli which we used minimized additional cues that may excite neuronal processes for motion or contour identification, allowing us to examine the stereoscopic processing per se. A variety of disparity stimuli have been used to identify the neural correlates of stereoscopic vision. Some had rich edge information (e.g., depth-defined checkerboard and center-surround disparity offsets) which were likely to induce neural processes related to contour-specific mechanisms, while some had slanted or curved surfaces, which contained geometric information for 3D shape processing (Anzai and DeAngelis 2010). When the stereoscopic cues appear in conjunction with other visual cues, different neural mechanisms may be engaged. For example, neurons in MT showed a weak selectivity to relative disparity, but only in the context of static visual signals (DeAngelis and Newsome 1999). When motion signals were introduced, transparent moving planes were able to evoke neural responses selective to the relative disparity signal in MT (Krug and Parker 2011). A systematic understanding of the causal roles of cortical areas in the depth-processing network remains to be a topic for future research.

Acknowledgements This work was supported by NSFC 31930053 and NSFC 31971031. We thank Siyuan Cheng for proofreading.

Author contributions All authors contributed to the study conception and design. Material preparation, data collection, and analysis were performed by NC and ZC. The first draft of the manuscript was written by NC and ZC. All authors revised the manuscript.

Funding This work was supported by NSFC 31930053 and NSFC 31971031.

Availability of data and material The data that support the findings of this study are available upon request.

Compliance with ethical standards

Conflict of interest The authors declare no conflicts of interest.

Ethics approval The experimental procedures and protocols have been approved by the human subject review committee of Peking University.

Consent to participate All subjects gave written, informed consent in accordance with the procedures and protocols approved by the human subject review committee of Peking University.

Consent for publication We confirm that we have given due consideration to the protection of intellectual property associated with this work and that there are no impediments to publication.

Code availability The codes for stimuli presentation of this study are available upon request.

References

Allen EA, Pasley BN, Duong T, Freeman RD (2007) Transcranial magnetic stimulation elicits coupled neural and hemodynamic consequences. Science 317(5846):1918–1921

Anzai A, DeAngelis GC (2010) Neural computations underlying depth perception. Curr Opin Neurobiol 20(3):367–375

Backus BT, Fleet DJ, Parker AJ, Heeger DJ (2001) Human cortical activity correlates with stereoscopic depth perception. J Neurophysiol 86(4):2054–2068

Brainard DH (1997) The psychophysics toolbox. Spat Vis 10(4):433–436

Cai P, Chen N, Zhou T, Thompson B, Fang F (2014) Global versus local: double dissociation between MT+ and V3A in motion processing revealed using continuous theta burst transcranial magnetic stimulation. Exp Brain Res 232(12):4035–4041

Carmel D, Walsh V, Lavie N, Rees G (2010) Right parietal TMS shortens dominance durations in binocular rivalry. Curr Biol 20(18):R799–R800

Chowdhury SA, DeAngelis GC (2008) Fine discrimination training alters the causal contribution of macaque area MT to depth perception. Neuron 60(2):367–377

Cocchi L, Sale MV, Lord A, Zalesky A, Breakspear M, Mattingley JB (2015) Dissociable effects of local inhibitory and excitatory theta-burst stimulation on large-scale brain dynamics. J Neurophysiol 113(9):3375–3385

Cottereau BR, McKee SP, Ales JM, Norcia AM (2011) Disparity-tuned population responses from human visual cortex. J Neurosci 31(3):954–965

Cumming BG, DeAngelis GC (2001) The physiology of stereopsis. Annu Rev Neurosci 24:203–238

DeAngelis GC, Cumming BG, Newsome WT (1998) Cortical area MT and the perception of stereoscopic depth. Nature 394:677–680

DeAngelis GC, Newsome WT (1999) Organization of disparity-selective neurons in macaque area MT. J Neurosci 19(4):1398–1415

Engel SA, Glover GH, Wandell BA (1997) Retinotopic organization in human visual cortex and the spatial precision of functional MRI. Cereb Cortex 7(2):181–192

Goncalves NR, Ban H, Sánchez-Panchuelo RM, Francis ST, Schluppeck D, Welchman AE (2015) 7 tesla FMRI reveals systematic functional organization for binocular disparity in dorsal visual cortex. J Neurosci 35(7):3056–3072

Huang Y-Z, Edwards MJ, Rounis E, Bhatia KP, Rothwell JC (2005) Theta burst stimulation of the human motor cortex. Neuron 45(2):201–206

Julesz B (1960) Binocular depth perception of computer-generated patterns. Bell Syst Tech J 39:1125–1162

Krug K, Parker AJ (2011) Neurons in dorsal visual area V5/MT signal relative disparity. J Neurosci 31(49):17892–17904

Kumar T, Glaser DA (1992) Depth discrimination of a line is improved by adding other nearby lines. Vis Res 32(9):1667–1676

Maunsell JH, Van Essen DC (1983) Functional properties of neurons in middle temporal visual area of the macaque monkey. II. Binocular interactions and sensitivity to binocular disparity. J Neurophysiol 49:1148–1167

Minini L, Parker AJ, Bridge H (2010) Neural modulation by binocular disparity greatest in human dorsal visual stream. J Neurophysiol 104(1):169–178

Neri P, Bridge H, Heeger DJ (2004) Stereoscopic processing of absolute and relative disparity in human visual cortex. J Neurophysiol 92(3):1880–1891

Parker AJ (2007) Binocular depth perception and the cerebral cortex. Nat Rev Neurosci 8:379

Parker A, Yang Y (1989) Spatial properties of disparity pooling in human stereo vision. Vis Res 29:1525–1538

Poggio GF (1995) Mechanisms of stereopsis in monkey visual cortex. Cereb Cortex 5:193–204

Preston TJ, Li S, Kourtzi Z, Welchman AE (2008) Multivoxel pattern selectivity for perceptually relevant binocular disparities in the human brain. J Neurosci 28(44):11315–11327

Qian N (1997) Binocular disparity and the perception of depth. Neuron 18:359–368

Roy JP, Komatsu H, Wurtz RH (1992) Disparity sensitivity of neurons in monkey extrastriate area MST. J Neurosci 12:2478–2492

Rutschmann RM, Greenlee MW (2004) BOLD response in dorsal areas varies with relative disparity level. NeuroReport 15(4):615–619

Sereno MI, Dale A, Reppas J et al (1995) Borders of multiple visual areas in humans revealed by functional magnetic resonance imaging. Science 268(5212):889–893

Tsao DY, Vanduffel W, Sasaki Y et al (2003) Stereopsis activates V3A and caudal intraparietal areas in macaques and humans. Neuron 39(3):555–568

Uka T, DeAngelis GC (2003) Contribution of middle temporal area to coarse depth discrimination: comparison of neuronal and psychophysical sensitivity. J Neurosci 23(8):3515–3530

Uka T, DeAngelis GC (2006) Linking neural representation to function in stereoscopic depth perception: roles of the middle temporal area in coarse versus fine disparity discrimination. J Neurosci 26(25):6791–6802

van Kemenade BM, Muggleton N, Walsh V, Saygin AP (2012) Effects of TMS over premotor and superior temporal cortices on biological motion perception. J Cogn Neurosci 24:896–904

Watson AB, Pelli DG (1983) QUEST: a Bayesian adaptive psychometric method. Percept Psychophys 33(2):113–120

Westheimer G (1979) Cooperative neural processes involved in stereoscopic acuity. Exp Brain Res 36(3):585–597

Westheimer G (1986) Spatial interaction in the domain of disparity signals in human stereoscopic vision. J Physiol 370:619–629

Wheatstone C (1838) XVIII. Contributions to the physiology of vision—part the first. On some remarkable, and hitherto unobserved, phenomena of binocular vision. Philos Trans R Soc Lond 128:371–394